INTERNATIONAL BACCALAUREATE
EXTENDED ESSAY
GROUP 4: PHYSICS

THE MAGNUS COEFFICIENT

NAME: JANA ŘEŽÁBKOVÁ
COUNTRY: CZECH REPUBLIC
SCHOOL: UWC RED CROSS NORDIC
WORD COUNT ESSAY: 3540
WORD COUNT ABSTRACT: 187

Abstract:

This essay aims to find out: **"How does surface roughness affect the magnitude of Magnus coefficient for a light low speed rotating cylinder?".** According to the boundary layer theory increase in surface roughness should lead to increase in the magnitude of Magnus force exerted on a rotating body and consequently to an increase in the Magnus coefficient, providing both the translational and angular velocity remain constant.

By creating a simple experimental setup, in which cylinders coated with different sized sandpapers were released from above and their landing was filmed and analyzed, a graph of Magnus coefficient against particle size corresponding to the used sandpaper grits was plotted.

Indeed an increasing trend in Magnus coefficient with increasing surface roughness was obtained. The magnitude of the Magnus Coefficient for used parameters corresponded to the accepted range of values. However, due to the imprecision of the experiment only relative change in magnitude was determined. The random errors were caused mainly by the release system, which was inducing rotational motion on the cylinder by twisting a string around its axis.

Overall the experiment was successful in answering the research question.

TABLE OF CONTENTS

Introduction:

Many people wonder how it is possible for a handball winger to score a goal directly from a corner. Or how does a center back manage to curve the ball around a wall of blocking players. In 1852 attention of German physicist Gustav Heinrich Magnus was caught by a very similar problem. Why don´t cannon balls flight straight when there is no wind? [A] He investigated the phenomenon now known as the Magnus effect. His work was later, in 1904, refined by another German engineer Ludwig Prandlt. His boundary layer concept now plays a prominent role in aerodynamics of sport balls. [B, 187]

The ever increasing competitiveness among professional players drives the research in the sport balls aerodynamics. From the effect of Reynolds number to the position of seams, sport balls are carefully examined in wind tunnels. The Adidas development team spent two and a half year on developing and testing the new Brazuca ball for the 2014 Football World Cup. [C]

This experimental investigation was inspired by the tennis rule enjoining the chair umpire to change balls every nine games, since hitting the balls alters the surface of the balls. This rule made me, as a huge tennis fan, wonder to what extent only a slight change in surface roughness influences the trajectory of the ball. Therefore this experiment aims to investigate the relationship between surface roughness and the Magnus coefficient.

For the purpose of this experiment the problem was simplified into 2-D by using a rotating cylinder. Also only low speed rotating bodies were used to avoid turbulent flow. Since aerodynamic forces act most markedly on light bodies [D, 174] care was taken to design the lightest cylinder possible. This led to the following research question:

How does surface roughness affect the magnitude of Magnus coefficient for a light low speed rotating cylinder?

Background Theory

Magnus Effect

The Magnus effect is a physical concept explaining and quantifying the force which acts upon translating spinning bodies. The force acts orthogonally to both the spin axis and the direction of motion. [D, 180]

From the definition it is clear that the force must be dependent on both angular velocity and translational velocity. The force should also be in some way dependent on the environment through which it is moving. Since real fluids are not inviscid and neither is the body ideally smooth viscosity plays a role in determining the magnitude of the force. Thus the Magnus force is directly proportional to fluid density and the size of the body, since increase in both

results in more fluid molecules colliding with the body and consequently increasing the force exerted on the body.

Mathematically the relationship for rotating cylinders could be described as follows: [D, 183] *(vector quantities are represented in bold, and left and up are positive directions)*

$$\mathbf{F_M} = C_M \rho R^2 \boldsymbol{\omega} \Lambda \mathbf{U} \quad (1)$$

where:
- $\mathbf{F_M}$ – force per unit length (N m^{-1})
- C_M – Magnus coefficient (used interchangeably with C_L the lift coefficient [H])
- ρ – the fluid density (kg m^{-3})
- R^2 – specific cross-sectional area (m^3)
- $\boldsymbol{\omega}$ – angular velocity (rad s^{-1})
- $\mathbf{U}$ – translational velocity (m s^{-1})

This investigation will deal solely with the Magnus coefficient and keep all the other variables determining the Magnus force constant. To understand the role of the Magnus force coefficient one must seek the explanation of the origin of the Magnus force.

The Boundary Layer

Because in reality conditions of inviscid fluid flowing around a smooth body cannot be created, the fluid molecules must be affected by the surface friction of the body. This leads to formation of a boundary layer firmly adhered to the body (Fig. 2). [A]

According to the boundary layer concept the fluid molecules in the boundary layer will accelerate on one side of the body, where the fluid velocity and the tangential velocity of the surface have the same direction, and decelerate on the other side, where the fluid velocity and tangential velocity of the surface oppose each other (Fig. 1). [A]

Since the further the fluid molecules are from the body´s surface the less affected they will be a velocity profile inside the boundary layer is created (Fig. 2). Boundary layer is defined as a region around the body where the velocity of fluid is within 99% of free stream velocity. [I, 2.4.2.]

Figure 1: The Formation of Boundary Layer, Illustrative

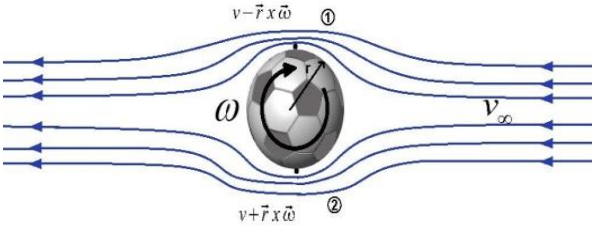

Figure 2: The Formation of Velocity Gradient, Illustrative

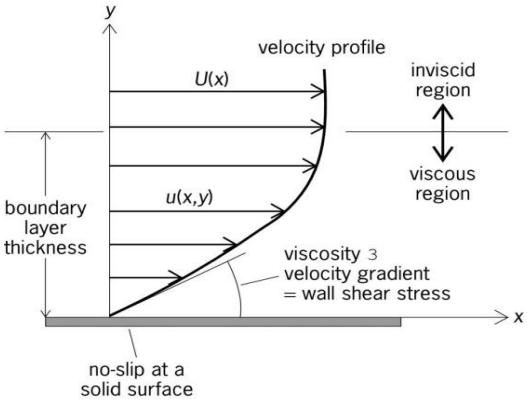

In accordance with the *Bernoulli principle* a pressure gradient corresponding to the velocity gradient (Fig. 2) will arise. Note that the pressure gradient inside the boundary layer doesn't vary with thickness. [E, 29] The pressure gradient therefore changes only in x-direction around the surface (Fig. 2).

The *Bernoulli principle* states that higher velocity implies lower pressure and vice versa. The difference in pressure results in a force in the direction from higher pressure region to lower pressure region. This force is called the Magnus force. Thus for the situation in Fig.1 Magnus force would have downward direction.

Magnus Coefficient

Magnus coefficient is a function of three variables: the Reynolds number, the spin parameter and surface roughness. [D, 182]

The Reynolds number can be calculated as: $Re = \mathbf{U}d / \nu$, where **U** is the velocity of the body, d is its diameter and ν is the kinematic viscosity of air. [B, 187]

The spin parameter is given as: $S = \boldsymbol{\omega}R / \mathbf{U}$, which is the relative ratio between angular and translational velocities. [D, 182]

Since both angular and translational velocity and the size of the cylinder will be kept constant throughout the experiment the effect of surface roughness on the magnitude of the Magnus coefficient can be investigated.

Boundary Layer Separation

The flow inside the boundary layer can be either laminar, turbulent or both. For low translational velocities and consequently low *Re* numbers (approximately less than 30 000) the boundary layer retains a subcritical flow regime characterized by laminar flow. [I, 3.1.1.] The predominant effect of changing surface roughness is the change in flow inside the boundary layer. [G, 25] In many sports additional surface roughness, such as dimples on the golf ball, can trigger the transition from laminar to turbulent flow on one side and thus increase the Magnus Force significantly. [B, 190] Generally the laminar boundary layer has lower momentum than turbulent boundary layer and it is therefore worse at withstanding the adverse pressure gradient [B, 187]. When boundary layer cannot withstand the adverse pressure gradient it tends to separate, or handle the pressure gradient later/earlier at opposing sides. [D, 177] The additional momentum on the retreating side of the body causes later separation/handling of the boundary layer compared to that on the advancing side, thus creating a wake deflected in the direction of the advancing side as depicted in Fig. 3. [B, 189] This wake exerts force on the fluid and thus according to *Newton´s 3rd Law of Motion*

the fluid will exert an equal and opposite force on the body – again the Magnus force. [B, 189]

Note that this explanation of Magnus force and the explanation using the *Bernoulli principle* both aid the Magnus effect. However the later explanation outweighs the *Bernoulli principle* explanation. This is most notable for smooth spheres where reverse Magnus effect is achieved. The reverse Magnus effect goes against the *Bernoulli principle*, but in accordance to flow separation. [D, 182]

Figure 3: Flow around a rotating tennis ball; Illustrative

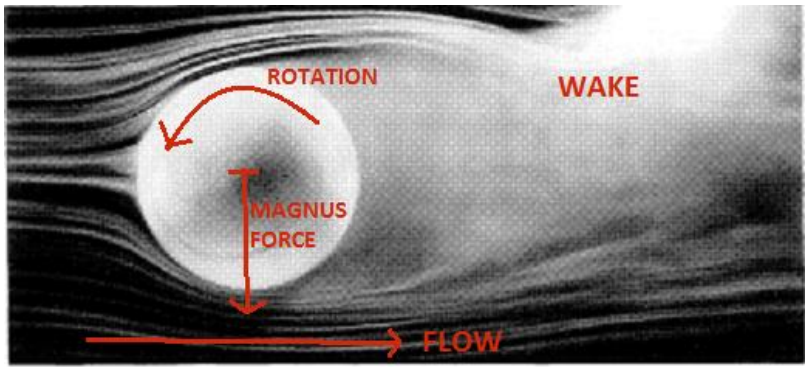

This experiment uses low speed cylinder in order to avoid triggering turbulent flow and thus encountering abrupt changes in the magnitude of the Magnus coefficient as in the case of golf balls. Therefore for the purpose of this experiment the flow in the boundary layer will be treated as laminar and the origin of the Magnus force will be considered the different handling of adverse pressure gradients inside the boundary layer caused by distinct velocity profiles and consequently pressure gradients for each surface roughness as suggested by the *Bernoulli principle*.

Experimental Method:

During the experiment cylinders coated with sandpaper were released from a ceiling with angular velocity induced by a string twisted around the cylinder's axis. The paths of the cylinders while landing were filmed with a reflex camera. The lateral deflections were then obtained by analyzing the footages.

Setup

The experiment was conducted in a laboratory using conventional materials. The design of the cylinder and the release system is especially noteworthy.

- **Cylinder**

The cylinder axis was mounted as seen in Fig. 4 using Lego components. It is detachable in the middle so that rolls coated with sandpaper can be inserted (Fig. 5). The sandpaper was wrapped around the paper roll using a strong tape.

Table 1: Materials used for cylinder design

Axis	1/2 Bush	4x
	Cross Axle Extension	1x
	Gear Wheel	2x
	Cross Axle	2x
Shell	Toilet Paper Roll	
	Sandpaper	

Figure 4: Design of the axis

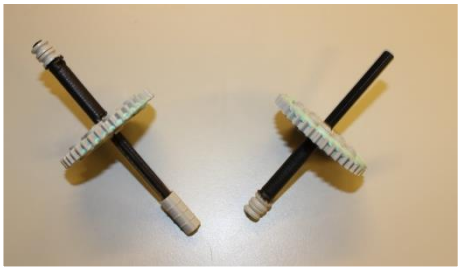

Figure 5: Cylinder coated with sandpaper

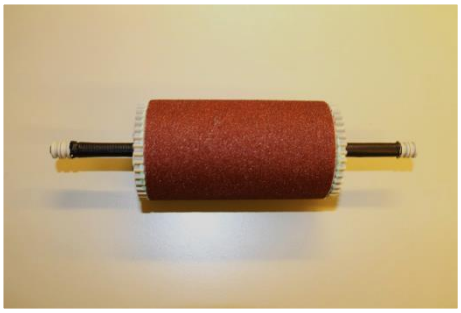

- **The Release System**

The angular velocity was induced on the cylinder by twisting a string around the axis. The string was in the form of loop loosely hanging on two hooks (Fig. 6). As the cylinder was placed on the string, the string bound in between the teeth of the gear wheel thus making it easy to twist the string around the axis. This design was employed since it yields the least rotation of the cylinder around vertical axis. Loosening the string at the top also improved the performance since it helps to balance the forces at each side of the string.

Figure 6: The release system for inducing rotation with a detail on the string fixation

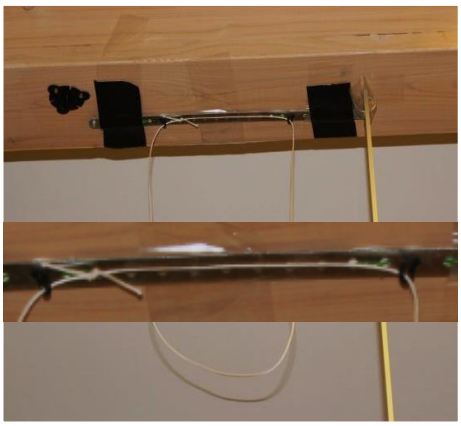

Measuring Surface Roughness

The surface roughness was varied by coating the cylinder using different types of sandpaper. To ensure that differences detectable by the setup were obtained a great range of sandpaper grits was used. The sandpaper grit type can be converted into particle sizes constituting the grit. Each sandpaper grit type with prefix P allows only a certain range of particle sizes within which more than 90% of the particles constituting the grit must be found. [F] The average particle size is then calculated and available online in conversion tables. It is the average particle size value that is used for the purpose of this investigation.

Table 2: Grit type/Particle size conversion [F]

Grit	Particle size (µm) ± 2
P80	201
P120	125
P150	100
P180	82
P240	59

Measuring Lateral deflection

The lateral deflection caused by the Magnus force was obtained by filming the landing of the cylinder on a table. A reflex camera with 55 fps video mode was used so that the footages could be analyzed using the VLC media player. Two rulers were placed perpendicularly to each other to measure the lateral deflection. One ruler marked a straight line from where the cylinder was released to the bottom table. There another ruler was used to measure the distance between the cylinder's axis and the vertical ruler. The measurement was done in Paint as it enabled to connect edges of the cylinder and determine their distance from the ruler (Fig. 7). The lateral deflection was obtained by calculating the mean of those edge values.

Figure 7: Example of video analysis; P120, Left Boundary: 12.0, Right Boundary: 18.0

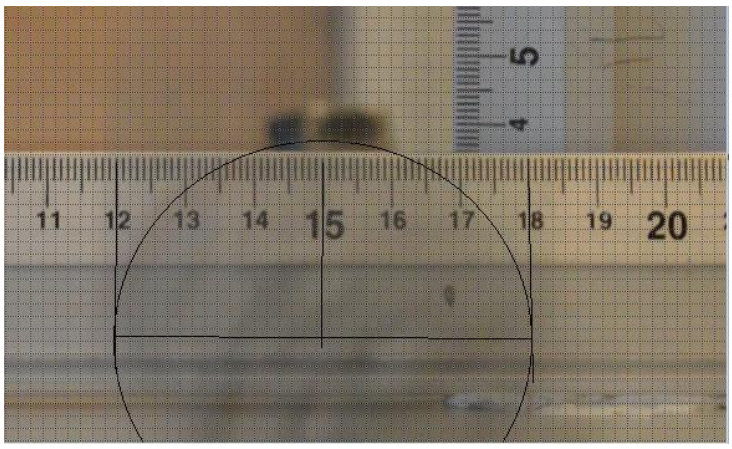

Assumptions and Controlled Variables

In this experiment following variables were controlled.

Translational velocity: The velocity was assumed to be controlled since the cylinder was falling from the same height and both the axle radius and the length of the string were constant. The role of surface roughness on the drag coefficient and thus the drag force was considered negligible. That is because as opposed to tennis ball the sandpaper coating is not fuzzy and porous – drag bearing. Therefore it does not experience varying pressure drags due to the varying lengths of porous fuzz. [B, 194]

This was verified by measuring the landing velocity for cylinders at the edges of used roughness spectrum. The velocities coincided within their uncertainty range.

Angular velocity: The angular velocity was calculated from translational velocity and as such is also controlled.

Mass of cylinders: The mass of cylinder was kept constant at 26.21 ± 0.01 g for all different surface roughnesses, so that the weight force was equal and did not cause differences in velocity. Where it was needed extra blu-tack was evenly added onto the gear wheels to match the mass but avoid shifting center of gravity.

The viscosity of air: The experiment was carried out at the same place and thus it is reasonable to consider the viscosity of air to be controlled.

Three assumptions were made while carrying the experiment.

The seam: Discrete roughness, such as the seam created by wrapping the sandpaper around the paper roll, and its position in relation to rotation also affects the Magnus force. [B, 195] This effect was assumed to have equal impact on the cylinders for all different surface roughnesses. To allow for the assumption the sandpaper was wrapped in the same way around the paper rolls and the seam was always aligned with the string when twisting the string in the release system.

The flow in boundary layer: remains laminar as mentioned in the background theory section.

The thin cylinder´s axis: doesn't affect the Magnus force. It was assumed that the Magnus force is caused only by the cylinder and thus its variation arises from the different surface roughness.

Results:

In the following tables (3 – 7) raw data from the experiment was recorded for each grit/surface roughness. Left and right bounds correspond to values read from the ruler that was positioned right behind falling cylinder (see Fig. 7). The uncertainty in the bounds was decided to be ± 0.2 cm due to the blurriness of the screenshots. Position of center value is the average of left and right bounds. The displacement of the cylinder, which was taken to be the displacement of its axis of rotation, was calculated using the following formula:

Displacement = (16.9 + 0.5) – Position of center

where, 16.9 cm was the value at which left edge of the vertical ruler crossed the horizontal ruler and 0.5 cm was the overlapping distance to the right between the left edge vertical ruler and the string release system.

The Average displacement is the mean of five values and its corresponding uncertainty is calculated as: 0.5*(MAX value – MIN value).

Table 3: Displacement measurement for grit P80

Left Bound (cm) ± 0.2	**Right Bound (cm)** ± 0.2	**Position of centre (cm)** ± 0.2	**Displacement (cm)** ± 0.2
10.8	17.3	14.1	3.4
11.6	18.2	14.9	2.5
11.0	17.9	14.5	3.0
11.0	18.2	14.6	2.8
11.3	17.7	14.5	2.9
Average displacement with uncertainty (cm):			2.9 ± 0.4

Table 4: Displacement measurement for grit P120

Left Bound (cm) ± 0.2	**Right Bound (cm)** ± 0.2	**Position of centre (cm)** ± 0.2	**Displacement (cm)** ± 0.2
12.2	17.6	14.9	2.5
12.0	18.0	15.0	2.4
11.5	17.5	14.5	2.9
12.3	18.7	15.5	1.9
12.0	19.2	15.6	1.8
Average displacement with uncertainty (cm):			2.3 ± 0.6

Table 5: Displacement measurement for grit P150

Left Bound (cm) ± 0.2	Right Bound (cm) ± 0.2	Position of centre (cm) ± 0.2	Displacement (cm) ± 0.2
12.4	17.2	14.8	2.6
12.1	18.8	15.5	2.0
12.4	18.3	15.4	2.1
12.0	18.0	15.0	2.4
10.6	18.9	14.8	2.7
Average displacement with uncertainty (cm):			2.3 ± 0.4

Table 6: Displacement measurement for grit P180

Left Bound (cm) ± 0.2	Right Bound (cm) ± 0.2	Position of centre (cm) ± 0.2	Displacement (cm) ± 0.2
12.1	18.4	15.3	2.2
12.3	18.3	15.3	2.1
11.8	18.5	15.2	2.3
12.5	19.2	15.9	1.6
11.0	17.5	14.3	3.2
Average displacement with uncertainty (cm):			2.2 ± 0.8

Table 7: Displacement measurement for grit P240

Left Bound (cm) ± 0.2	Right Bound (cm) ± 0.2	Position of centre (cm) ± 0.2	Displacement (cm) ± 0.2
12.1	18.0	15.1	2.4
12.0	18.6	15.3	2.1
12.7	19.2	16.0	1.5
12.5	19.4	16.0	1.5
12.4	18.6	15.5	1.9
Average displacement with uncertainty (cm):			1.9 ± 0.5

Graph 1: Displacement against grit size for all runs

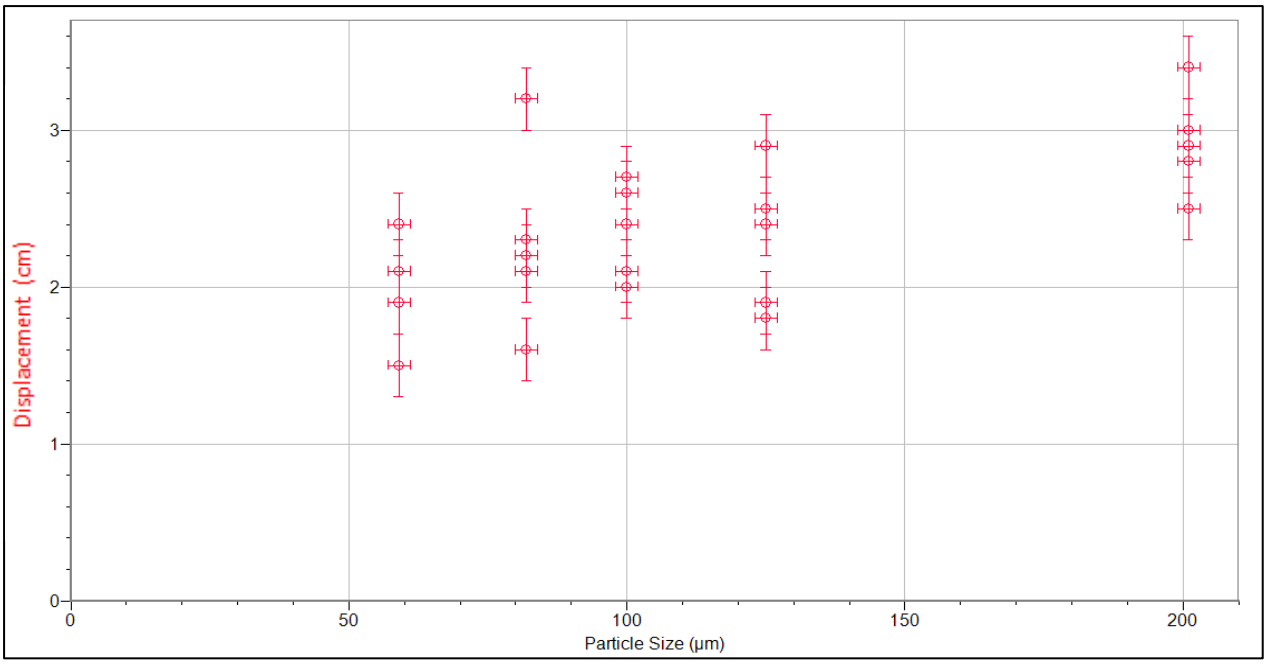

From Graph 1 it is clear that this experiment deals with random errors and hence low precision. However it can be observed that the upper range sandpaper grit P80 (particle size 201 ± 2 μm) has distinctly higher displacement values than the lower range sandpaper grit P240 (particle size 59 ± 2 μm).

To represent the average displacement values as forces needed to displace the cylinder during the flight a video of the whole experiment was analyzed using LoggerPro. This was done for both P80 and P240 grits to represent the whole roughness spectrum and find potential differences in velocity or time taken for the free flight. Since the results for both times taken and velocities were within 0.01 for both grits in the analyzed videos, differences were considered to be negligible. The distance between top and bottom in the experiment is 1.600 ± 0.005 m.

Graph 2: Velocity/Time graph

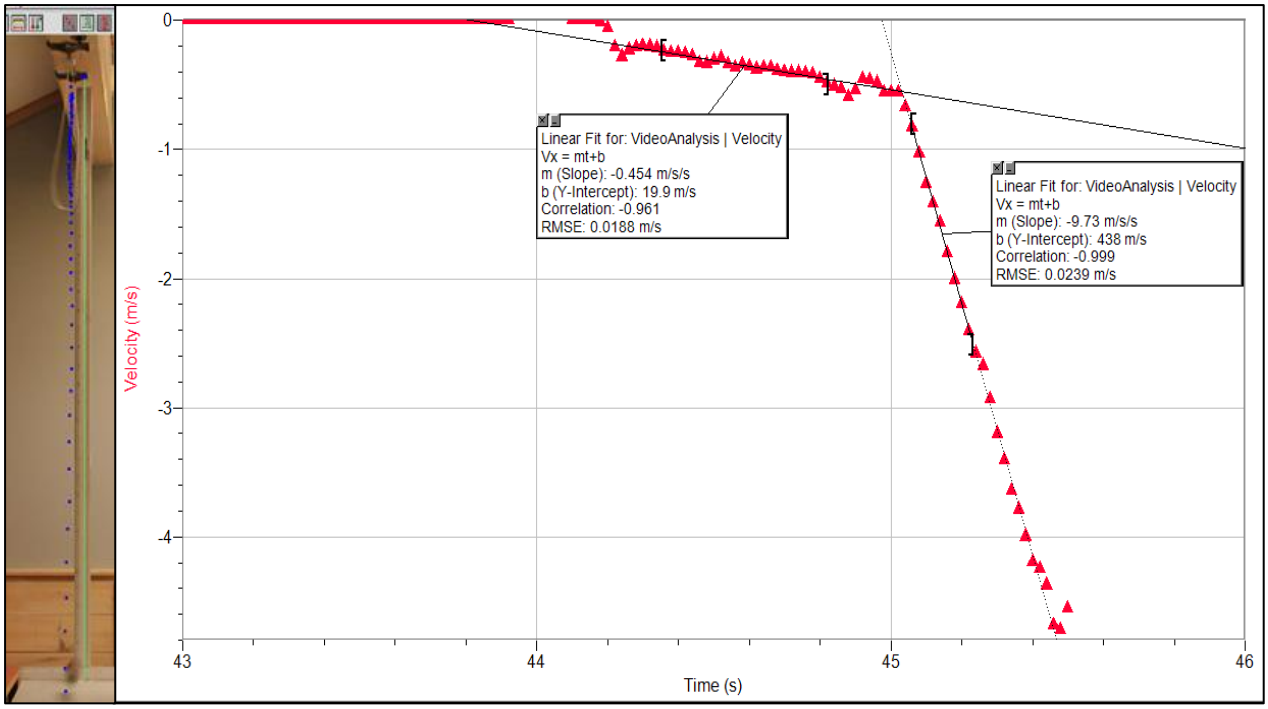

From the graph those values can be obtained:

Cylinder untwisting:

Acceleration: 0.454 ± 0.001 m s^{-2}

Final velocity: 0.559 ± 0.001 m s^{-1}, value is specified in the graph´s table

Cylinder´s free flight:

Acceleration: 9.73 ± 0.01 m s^{-2}

Final velocity: 4.69 ± 0.01 m s^{-1}, value is specified in the graph´s table

Therefore time taken for free flight is equal to change in velocity/acceleration.

t = (4.69 - 0.559) / 9.73 = 0.425 ± 0.002 s

Since during the time the cylinder untwists from the string the Magnus force acts against horizontal component of tension and the cylinder has low translational velocity it is assumed that no horizontal displacement is achieved.

Thus the horizontal acceleration is calculated using following formula: **a** = (2 * **s**) / t^2 , where time is 0.425 s and **s** are respective average displacements from the experiment.

Horizontal force is simply the product of acceleration and cylinder´s mass (26.21 ± 0.01 g).

The horizontal force values for all grits have to be divided by the cylinder´s length since $\mathbf{F_M}$ in the Magnus force formula is force per unit length. (Length of cylinder: 0.0820 ± 0.0005 m)

Table 8: Force/Displacement conversion

Grit	Average Displacement (m)	Unc. Average Displacement (m)	Force (N)	Force/Length (Nm^{-1})	Unc. Force/Length (Nm^{-1})
P80	0.029	0.004	0.0084	0.10	0.01
P120	0.023	0.006	0.0067	0.08	0.02
P150	0.023	0.004	0.0067	0.08	0.02
P180	0.022	0.008	0.0064	0.08	0.03
P240	0.019	0.005	0.0055	0.07	0.02

The uncertainty in Force/Length was calculated as the sum of relative uncertainties of: average displacement, mass, time[2] and length of cylinder.

Value of constant variables:

Radius of cylinders base: 0.0210 ± 0.0005 m

Air density: 1.194 kg m^{-3} [J], (at sea level when T = 20°C and relative humidity is 60%)

Velocity: 4.69 ± 0.01 m s^{-1}

Angular velocity: 223 ± 6 rad s^{-1} , calculated from formula $\boldsymbol{\omega} = \mathbf{U}/R$

Uncertainties are taken from the measuring devices. Uncertainty for angular velocity is the sum of relative uncertainties for radius and velocity.

The formula for calculating Magnus force is: $\mathbf{F_M} = C_M \rho R^2 \boldsymbol{\omega} \Lambda \mathbf{U}$
Thus the constants plugged into the equation give: $\rho R^2 \boldsymbol{\omega} \Lambda \mathbf{U} = 0.552 \pm 0.04$

Magnus coefficient is the quotient of $\mathbf{F_m}/(\rho R^2 \boldsymbol{\omega} \Lambda \mathbf{U})$

Table 9: Magnus coefficient for each surface roughness

Grit	Particle size (µm) ± 2	Magnus Coefficient	Unc. C_m
P80	201	0.19	0.04
P120	125	0.15	0.05
P150	100	0.15	0.04
P180	82	0.14	0.06
P240	59	0.12	0.04

The uncertainty in Magnus Coefficient was calculated as the sum of relative uncertainties of: force/length and the uncertainty of constant term.

Graph 3: Magnus coefficient /Particle size graph

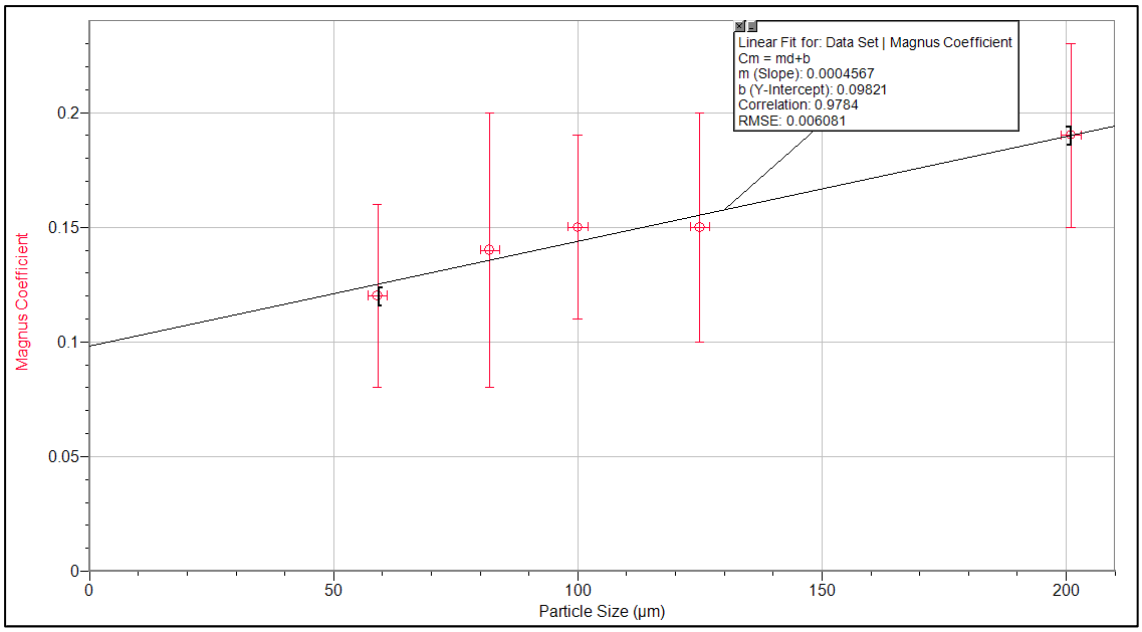

Despite the high uncertainties a general trend of increasing Magnus coefficient with increasing surface roughness can be seen. This corresponds to the theory that the boundary layer forms around the body due to surface friction and thus increasing surface roughness increases the velocity gradient, which consequently increases the pressure gradient and thus the Magnus force. However, a further description of this trend cannot be made due to the uncertainty.

The calculated magnitude of Magnus coefficient from this experiment coincides with the accepted range of values of Magnus coefficient for used spin parameter and Reynolds number. Figure 8 represents a graph of lift coefficient (Magnus coefficient) against the ratio of circumferential to free stream velocity (α) for different surfaces at various Reynolds numbers. In this experiment the circumferential and free stream velocities were equal and *Re* equaled approximately 12.5k, which is lower than the *Re* of curves in Figure 8. In Figure 8 it can be seen that all function curves cross $\alpha = 1$ at values $C_L < 1$, which coincides with the results of this experiment.

Figure 8: Surface roughness effect on the lift coefficient according to Thom

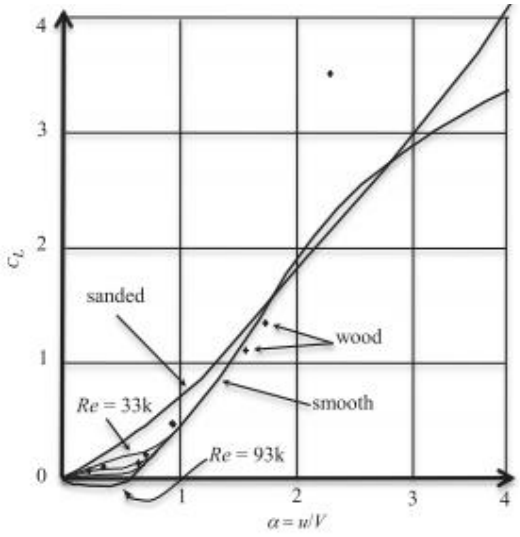

Discussion:

Although the investigation confirmed that as surface roughness increases the Magnus coefficient tends to increase, this experiment is too imprecise to provide any further conclusion. Excluding the uncertainty of used measuring devices, there was one major source of random error.

The problem of string twisting was probably responsible for the random error in displacement values. Although the designed release system minimized the rotation along other than central axis, it can still be seen that the difference between left and right bounds in the analyzed snapshots exceeds the actual diameter of 4.2 cm and is mostly in the range of six to seven centimeters. This was partially due to the blurriness of the snapshots (this could be potentially improved by attempting to focus the camera on the cylinder instead of the rulers); however, it also suggests that there was extra rotation not taken into account. This rotation was most likely caused by the unsymmetrically twisted string on opposing sides of the cylinder. This resulted in differences for each run. Also as the cylinder was being released the retreating hand could have pushed it slightly to the side.

It must also be acknowledged that the sand paper grits used differed in their particle size only by tens of micrometers, since it was the greatest range allowed to keep the cylinder light enough to detect differences in the Magnus force (this was experimentally confirmed). The choice of grits was aimed to be representative of the slight surface alternations a set of tennis balls would probably undergo during nine games before being changed. Therefore it makes sense that the displacements for different grits didn´t differ substantially. However, in tennis itself the difference would be magnified since both translational and angular velocities are many times higher than in this investigation.

The experiment was also based on the assumption that the seam affects all cylinders during all runs equally. However, since the random error in displacement was most likely due to unsymmetrically twisted string, the control of the seam by positioning it in the same way along the string for all runs could no longer be considered effective enough. Thus the seam also enhanced the random error in displacement values.

Conclusion:

This investigation aimed to explore the following research question:

How does surface roughness affect the magnitude of Magnus coefficient for a light low speed rotating cylinder?

By using a simple experimental setup the magnitudes of Magnus coefficient for five different surface roughnesses were obtained. The values indicate that increase in surface roughness leads to increase in magnitude of Magnus coefficient for a light low speed rotating cylinder. This trend corresponds to the theory as presented in the background theory section.

Main problem of this experiment was the insufficient control of random errors. Simplicity and use of conventional materials was prioritized on the expanse of more extensive control over the experiment. Hence, only relative change in the magnitude of Magnus coefficient for a light low speed rotating cylinder for different surface roughnesses was determined.

This experiment illustrates the important role of physics in sports. Many experiments could serve as extension to this investigation. Since the idea of this experiment was sparked by tennis balls change rule, it would also be interesting to investigate another tennis rule: at Wimbledon, one of the Grand Slam tournaments, balls have to be stored in refrigerator at constant temperature of 20°C [K]. Therefore it raises a question of "how does temperature affect trajectory of tennis balls?" Those could include bouncing or effect if any on Magnus force. It would also be interesting to simulate the same conditions (*Re*, S) as in this experiment inside a wind tunnel and compare the results.

Bibliography:

(A) REICHL, Jaroslav. 2006 – 2014. Magnusův jev. *Encyklopedie Fyziky* [online]. Retrieved on 17.11.2014, from http://fyzika.jreichl.com/main.article/view/556-magnusuv-jev (Own translation from Czech)

(B) MEHTA, R. D., & PALLIS, J. M. 2001. Sports Ball Aerodynamics: Effects of Velocity, Spin and Surface Roughness. *Materials and Science in Sports* [online]. 185 – 197. Retrieved on 17.11.2014, from http://iweb.tms.org/ED/01-5085-185.pdf

(C) SALTER, Chuck. 2013, December 3. Adidas reveals the Brazuca, a world cup soccer ball two and a half years in the making. *FastCompany* [online]. Retrieved on 17.11.2014, from http://www.fastcompany.com/3022879/adidas-reveals-the-brazuca-a-world-cup-soccer-ball-two-and-a-half-years-in-the-making

(D) BUSH, J. W. M. 2013. The aerodynamics of the beautiful game [online]. 171 – 192, MIT. Retrieved on 17.11.2014, from http://math.mit.edu/~bush/wordpress/wp-content/uploads/2013/11/Beautiful-Game-2013.pdf

(E) FIELDING, Suzanne. Laminar Boundary layer separation [online]. 28 – 30, Durham University. Retrieved on 17.11.2014, from http://community.dur.ac.uk/suzanne.fielding/teaching/BLT/sec4c.pdf

(F) Sandpaper (coated abrasives) - Grades [online]. Retrieved on 17.11.2014], from http://sizes.com/tools/sandpaper.htm#Standards

(G) SEIFERT, Jost. 2012. A review of the Magnus effect in aeronautics. *Progress in Aerospace Sciences* [online]. 55, 17 – 45. Retrieved on 17.11.2014, from http://www.see.ed.ac.uk/~shs/Climate%20change/Flettner%20ship/Seifert%20Flettner%20apps.pdf

(H) GUZZELA, L., & RIENER, R. 2007 - 2008. Bend it Project [online]. Swiss Federal Institute of Technology Zurich. Retrieved on 17.11.2014, from https://www.rdb.ethz.ch/projects/project.php?proj_id=21453&z_detailed=1&z_popular=1&z_keywords=1

(I) CHKLOVSKI, Tara. Pointed-tip wings at low Reynolds numbers [online]. Lodz University. Retrieved on 17.11.2014, from http://www.wfis.uni.lodz.pl/edu/Proposal.htm#_Toc110650477

(J) Air Density Calculator [online]. Retrieved on 17.11.2014, from http://www.denysschen.com/catalogue/density.aspx

(K) Having a ball at Wimbledon! [online] Retrieved on 17.11.2014, from http://news.bbc.co.uk/sportacademy/hi/sa/tennis/features/newsid_2997000/2997504.stm

Image Sources:

Figure 1:

https://www.rdb.ethz.ch/projects/project_image_full.php?proj_id=21453&exit=1&pi_id=12240 (Retrieved on 12th Oct 2014)

Figure 2:

http://encyclopedia2.thefreedictionary.com/_/viewer.aspx?path=mgh_cep&name=Typical-laminar-boundarylayer-velocity-profile.jpg (Retrieved on 12th Oct 2014)

Figure 3:

http://iweb.tms.org/ED/01-5085-185.pdf (Page 189, retrieved on 12th Oct 2014)

Figure 8:

http://www.see.ed.ac.uk/~shs/Climate%20change/Flettner%20ship/Seifert%20Flettner%20apps.pdf (Page 25, retrieved on 12th Oct 2014)